An Edge Embedded Marker-Based Watershed Algorithm for High Spatial Resolution Remote Sensing Image Segmentation

Deren Li, Guifeng Zhang, Zhaocong Wu, and Lina Yi

***Abstract*—This correspondence proposes an edge embedded marker-based watershed algorithm for high spatial resolution remote sensing image segmentation. Two improvement techniques are proposed for the two key steps of maker extraction and pixel labeling, respectively, to make it more effective and efficient for high spatial resolution image segmentation. Moreover, the edge information, detected by the edge detector embedded with confidence, is used to direct the two key steps for detecting objects with weak boundary and improving the positional accuracy of the objects boundary. Experiments on different images show that the proposed method has a good generality in producing good segmentation results. It performs well both in retaining the weak boundary and reducing the undesired over-segmentation.**

***Index Terms*—Edge embedded, high spatial resolution, image segmentation, marker-based watershed, remote sensing.**

I. Introduction

High spatial resolution remote sensing image (HSRI) provides much structural detail of ground objects for mapping and monitoring the earth surface at local scale. With the spatial resolution refinement, the internal variability within homogenous land cover units increases, object-based image analysis becomes the first choice for HSRI application recently [1], [2]. As a fundamental process, HSRI segmentation is essential for the latter image analysis. It partitions the images into un-overlapping homogenous regions or objects [3]. The quality of the extracted object boundaries plays a key role for the overall efficiency of the feature extraction [4] or classification [5], [6]. It is needed to develop effective and efficient image segmentation approach to extract accurate object boundaries from HSRI.

In past few decades, various segmentation techniques have been proposed. Generally, they are based upon two basic properties: similarity and discontinuity. Pixel similarity gives rise to region-based segmentation [7]–[9], whereas pixel discontinuity gives rise to edge-based segmentation [10]–[12]. These two traditional techniques may be able to get good result for some simple images. However, it is always difficult to achieve desired result for HSRI segmentation due to the complexities of the landscape structure on the image. While textures in objects, such as forest, are always detected as spurious object boundaries which causes over-segmentation; the edges between the farm fields may appear to be obscure that may induce under-segmentation.

Manuscript received January 14, 2010; revised April 02, 2010; accepted April 02, 2010. Date of publication May 03, 2010; date of current version September 17, 2010. This work was supported in part by the National Natural Science Foundation of China under Grants 40201039 and 40771157, by the National High Technology Research and Development Program of China under Grant 2007AA12Z143, and by the Fundamental Research Funds for the Central Universities under Grant 20082130201000048. The associate editor coordinating the review of this manuscript and approving it for publication was Dr. Brian D. Rigling.

D. Li is with the State Key Laboratory of Information Engineering in Surveying, Mapping, and Remote Sensing, Wuhan University, Hubei 430079, China.

G. Zhang is with the Academy of Opto-Electronics, Chinese Academy of Science, Beijing 100080,China (e-mail: russhome@126.com).

Z. Wu and L. Yi are with the School of Remote Sensing and Information Engineering, Wuhan University, Hubei 430079, China.

Digital Object Identifier 10.1109/TIP.2010.2049528

With regard to these problems, many works have been done. Some researchers integrated texture in segmentation to avoid the over-segmentation of spectral heterogeneous objects [13]. In this strategy, the texture calculation before segmentation is time-consuming. Moreover, the texture boundary effect [14] may induce the location uncertainty of the extracted object boundaries. Some researchers proposed to segment image at multiscale, then select and merge the optimal scale of segmentations to achieve good result [15]. However, how to select the optimal scale for different type of ground objects and merge them is still a difficult task that needs further research. Some researchers tried to integrate edge information into segmentation to get more accurate object boundaries [16]. This strategy takes the advantage of both region-based and edge-based segmentation techniques and is more practical for the quick and effective processing of large size data.

This correspondence follows the edge integration strategy and proposes an edge embedded marker-based watershed algorithm (EEMW) for high spatial resolution remote sensing image segmentation. Edges detected by the edge detector embedded with confidence [17] is integrated into the two steps of marker-based watershed segmentation, namely the extraction of markers and the labeling of pixels. Moreover, an adaptive maker extraction method is proposed and implemented. This method takes into account the complexity of grey level distribution of different objects on HSRI. The extracted makers are more coincide with the inner regions of ground objects. To meet the application requirement of efficient large HSRI processing, the scheme of labeling pixels in literature [18] is implemented. It was developed based upon the pixel labeling scheme of Meyer's algorithm [19]. Instead of using the hierarchical circular queues [19], a data structure with one queue and one stack is used in the pixel labeling process [18]. Therefore, it can largely save memory cost and be applied to large size images.

The rest of the correspondence is organized as follows. Section II clarifies the basic concepts in the EEMW segmentation and gives an overview of the proposed method. Section III illustrates the implementation method of the EEMW segmentation algorithm from two aspects: the marker extraction and the labeling of the pixels. Section IV describes the experiments of Quickbird image and compared the segmentation results by the proposed method and the H-minima algorithm [1]. Section V summarizes the results and draws conclusions.

II. Framework of EEMW Segmentation Method

Freixenet *et al.* surveyed the technique of region and boundary information integration for segmentation and categorized the methods into two classes: the embedded integration and postprocessing integration [16]. The embedded integration methods integrate edge information through the definition of new parameters or a new decision criterion for segmentation [12], [20]–[23]. In the postprocessing integration methods [24]–[28], edge and region information are extracted independently as a preliminary step, then a posterior fusion process tries to exploit the dual information in order to modify, or refine the segmentation. The proposed method belongs to the embedded integration method. The edge information is integrated into the two key steps of marker-based watershed segmentation algorithm.

A. Edge Detection With Embedded Confidence

The edge information is detected by the confidence embedded edge detection method [17]. In the method, an independent measure of confidence is estimated in the presence of the employed edge model. The widely used three-step edge detection procedure: gradient estimation,

nonmaxima suppression, hysteresis thresholding is generalized to include the information provided by the confidence measure. It is particularly effective in detecting weak edges without introducing spurious edges.

The confidence measure η is defined as the absolution value of the cosine of the angle between the normalized unit vector of the data a and an ideal template t. Because both the data and the template are not in the gradient space, η provides an independent estimate for the presence of the assumed edge model. Interpreted in the image domain, η measures the similarity between the normalized data and the template.

The procedure of the method can be briefly described as follows. First, the value of the gradient magnitude g and orientation θ is estimated. The normalized gradient magnitude ρ is defined from the cumulative distribution of g. For each pixel the two independent measures of ρ and η are used to define a $\rho\eta$-diagram. Then the nonmaxima suppression and hysteresis thresholding are implemented based upon the $\rho\eta$-diagram.

Let $f(\rho, \eta) = 0$ be the implicit equation of a curve in the ρ-η plane. For any point (ρ^0, η^0), the value $f(\rho^0, \eta^0)$ is called the algebraic distance (AD) of the point from the curve. The AD of a point on the curve is zero. The sign of the AD divides the plane into two regions.

In the nonmaxima suppression, the pixel is a local maximum only when both virtual neighbors have negative ADs. Only the local maximum pixels are retained in the latter processing.

In hysteresis thresholding, two decision boundaries of the lower boundary $f^{(L)}(\rho, \eta) = 0$ and the higher boundary $f^{(H)}(\rho, \eta) = 0$ can be defined in the $\rho\eta$-diagram. For each pixel (ρ^0, η^0), the AD of the point from the curve $f(\rho^0, \eta^0)$ is used instead of the gradient magnitude thresholds in Canny algorithm [10]. Since pixels of weak edges mainly locate in the up-left corner of the diagram, the weak edges can be completely detected without introducing the spurious edges if the suitable threshold curves are defined.

B. Marker-Based Watershed Segmentation

Watershed algorithm [29] is usually applied to the gradient image [30]. Imagine the gradient image is a topographic surface, a hole is drilled in each minimum of the surface, and water is flooded into different catchment basins from the holes. As a result, the water starts filling all catchment basins, which have minima under the water level. If two catchment basins would merge as a result of further immersion, a dam is built all the way to the highest surface altitude and the dam represents the watershed lines. This flooding process will eventually reach a stage when only the top of the dam is visible above the water line. The result is a tessellation of the input image into its different catchment basins, each one characterized by a unique label [31].

The method is a two-stage process, including the extraction of marker image and the labeling of pixels (flooding). Markers are a set of components marking flat regions of an image, i.e., each marker indicates the presence of an object. If the object interiors (markers) are set to 1, and the uncertainty areas are set to 0, we get a binary marker image. It contains a set of components (markers) marking the core regions, and a large number of pixels may remain unassigned. The next step is then to label the unassigned pixels by the extended watershed algorithm dealing with markers to get the final partition. It has the advantage that segmented results can have coherent regions, link edges, no gaps due to missing edge pixels. However, applying this method to HSRI segmentation, the noises or textures on the image are usually labeled as the pseudo-local minimum regions and result in over-segmentation.

To reduce over-segmentation, we make some improvements to the marked-based watershed segmentation algorithm [18]. First, a regional adaptive marker extraction method is proposed. The marker image is created from gradient image by binary processing. Instead of using a fixed threshold, such as H-minima algorithm [1], a threshold image, on which the threshold of each pixel is statistically estimated and used for binarization. Because it considers the complex grey level distribution of HSRI, the extracted makers are more coincide with the real objects. Then, the image labeling scheme in the Meyer's algorithm is implemented by using one queue and one stack data structure. This scheme can largely save memory cost and make it applicable to large image.

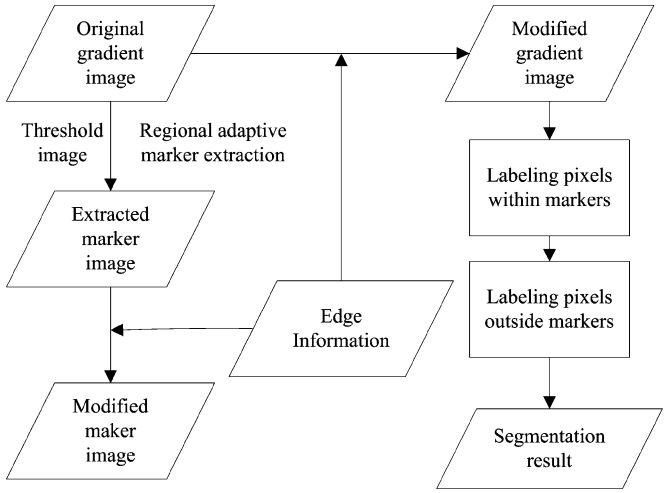

Fig. 1. Framework of EEMW segmentation.

C. Scheme of Integrating Edge Information

In most of the research, the edge information should be tracked before using them to guide the segmentation. It is time consuming and will reduce the segmentation efficiency. This correspondence proposed a edge embedded algorithm which need not track the edges. The intention of this algorithm is to promote the segmentation efficacy as well as to ensure most of the boundaries acquired by segmentation be consistent with the edges obtained.

With consideration that object edges can not pass through the markers, the marker image is rectified according to the edge information to get the final marker image that is more appropriate to the reality.

In labeling pixels, pixels are more possible to become the pixels on watershed line if they are lastly labeled. Therefore, we assign pixels on the edges the lowest priorities and processed lastly. Since the processing priority of pixel is defined as the reciprocal of its gradient magnitude, the gradient image is rectified according to edge information in advance. In the process, the pixels within markers are labeled by the region growing method first and then the other pixels outside the markers are labeled according to the rule that two pixels must not be labeled with same region ID if their common neighboring pixels are all the edge pixels. The overall framework is shown in Fig. 1.

III. Implementation Method of EEMW Algorithm

As shown in Fig. 1, the edge information is used to modify the maker image and direct the labeling of pixels within/outside markers by rectifying the gradient image in advance.

A. Marker Extraction

In HSRI, there are various land cover objects with different texture granulations. The gradient magnitudes (GM) of pixels are intricately distributed. The GM of pixels within the homogenous object are commonly lower than that of the boundary pixels. This make it possible to

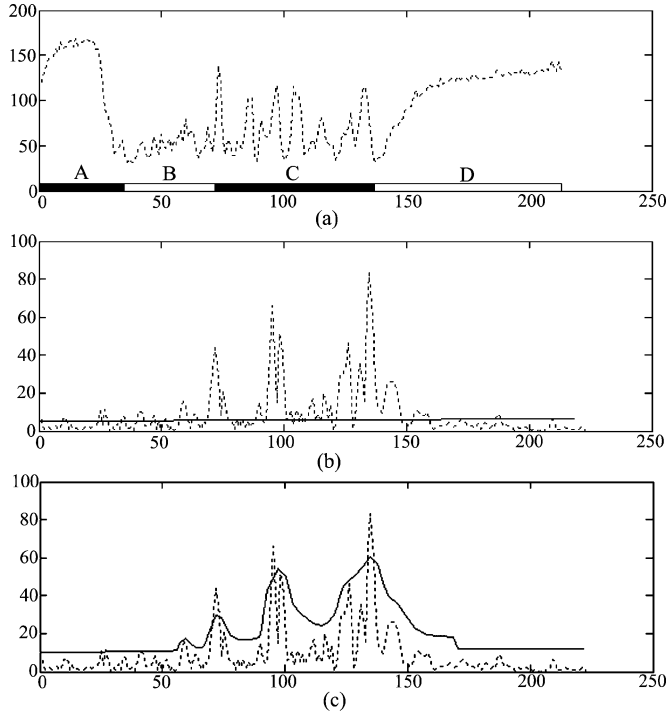

Fig. 2. Extracting marker image with a binary processing method for: (a) a 1-D signal curve (dotted line) with object A, B, C, and D, (b) gradient magnitude curve (dotted line) and a fixed threshold (solid line), (c) gradient magnitude curve (dotted line) and the estimated threshold curve (solid line).

set a threshold to binalize the gradient image to get makers. However, the GM of pixels in the object with complex texture may be comparable or ever higher than that of the boundary pixels. It will fail to extract correct marker image with a single threshold in binarization.

Hence, augmenting the marker image extraction is paramount. We propose a regional adaptive marker extraction method, instead of using a single threshold, a threshold image (TI) is estimated. Let GI represent the gradient image, then the marker image is defined as a binary image (BW) that is the result of the logical operation: $\mathrm{BW} = \mathrm{GI} < \mathrm{TI}$. Fig. 2(a) shows a 1-D signal with four distinct objects. The grey value of pixels within object B and C varies greatly. Hence, the gradient magnitude of pixels in these objects is high [Fig. 2(b)]. Setting a single fixed threshold will fail at extracting the appropriate markers. A too low threshold yields too many markers and leads to over-segmentation [Fig. 2(b)]. However, using an estimated threshold curve, which is a 1-D TI, allows the extraction of the desired five markers [Fig. 2(c)].

The estimation of TI is the key for extracting good markers. In the process, the low-pass component of the gradient image (LCG) is first calculated by the Butterworth low-pass filter, which is capable of avoiding obvious ringing phenomenon [1]. LCG corresponds to the main contents of the gradient image. On LCG, the high gradient value of texture and noises can be largely suppressed, the pixels with high values are always on sharp edges and the pixels with low values are on weak edges or in the objects. Therefore, the LCG can be used to direct the threshold setting. Multiply the LCG with an appropriate scale factor (T, [0–1]), the result image is especially useful for the marker extraction of objects with textures, such as the object B and C in Fig. 2(a). However, for the homogenous object, such as object A and D in Fig. 2(a), the scaled LCG may be too low and leads to over-segmentation. For such objects, we suggest using an empirical statistic threshold (EST) as the threshold. The EST value for a certain image is defined as the α fractile of the gradient level probability distribution. α ranges from [0–1]. With a defined α, the accumulated proportion of pixels with the gradient value lower than EST equals to α. Therefore, for each pixel on TI, the corresponding scaled LCG value is compared with the EST value, the maximum between them is defined as the pixel value.

Then, markers in BW with insufficient spatial support are rejected as these markers are usually caused by noise. We set an appropriate area threshold (A) to remove these markers. For a given spatial resolution remote sensing image, A equals to the area of the smallest discernable object.

Finally, the pixels of markers should be within the objects, the edge pixels should not be within markers. Under the direction of edge information, we assign value 0 to each edge pixel on BW. The updated BW is taken as the final marker image. In summary, the marker extraction process can be described as:

Algorithm III-A

- marker image extraction

  T: scale factor

  A: the appropriate area threshold

  n: number of the pixels

  α: significant level

Steps:

i) Get LCG from GI with a Butterworth low-pass filter
ii) Generate gradient image histogram (H)
iii) Compute probability $P(i)$ of each gradient level i

$$P(i) = H(i)/n$$

iv) Compute EST
v) Generate TI

$$\mathrm{TI} = \max(\mathrm{LCG} \times T, \mathrm{EST})$$

vi) Binarize GI with TI to get BW

$$\mathrm{BW} = \mathrm{GI} < \mathrm{TI}$$

vii) Remove small regions
if the area of region in $\mathrm{BW} < A$ **then**
Assign each pixel in the region value 0 on BW
end if
viii) Rectify BW according to the edge information

In the algorithm, the setting of parameter directly impact the final segmentation result. The appropriate parameter values should be chosen according to the requirement of specific segmentation task. With regard to the setting of parameters, the lower the α is, the less the object inner pixels are marked. If α is set lower than the appropriate value, the result tends to be over-segmentation. But if α is set higher than the appropriate value, the result tends to be under-segmentation. Generally, we select α in the value range of [0–0.7]. The appropriate area threshold A equals to the area of smallest discernable object on the image. If the area threshold is set lower than A, the small markers caused by noises or texture leads to over-segmentation. But if the area threshold is set higher than A, the removal of real markers leads to under-segmentation. Finally, the change of parameter T induces different marker extraction results for different types of objects. Given an appropriate parameter α is set, for the textured objects, the lower the T is, the less the object inner pixels are marked, the more the markers are extracted, which leads to their over-segmentation, vice versa; however, for the homogenous objects, the lower the T is, the

more the object inner pixels are marked, the less the markers are extracted, which may lead to their under-segmentation, vice versa. We suggest to set T in the range [0.6–0.7].

B. Labeling Pixels

The labeling of pixels is the process of assigning each pixel a unique identity (ID). There are two often-used pixel labeling methods. 1) The first method uses the individual markers as the local minima in the gradient image. It filters out the undesired minima of the gradient image, and applies the traditional watershed segmentation on the revised gradient image. 2) The second method suppresses unwanted minima during labeling process [19].

The marker based immersion type watershed algorithm proposed in literature [19], performs the flooding process directly on the original gradient image. It was realized by using the data structure of hierarchical circular queues. The hierarchical circular queues are a set of queues with different priorities, each queue is a first-in first-out data structure. The priority of each pixel in the gradient image is defined as the reciprocal of its gradient value. This implies that a high (low) priority is assigned to a pixel with low (high) grey-level value. To save memory cost for large image segmentation, we proposed to use a data structure of only one queue and one stack to store the temporary data in image labeling [18]. It can largely reduce the memory cost.

The pixels are first sorted in an descending order of priority. Then the possible neighbor labeled pixel of each unlabeled pixel is searched by seed tracing to identify the label ID for the current processing pixel. In the search process, one queue (QU) and one stack (ST) are used. In labeling pixels, the pixels within marker and the pixels outside makers are labeled successively.

C. Labeling Pixels Within Markers

This step is realized by seed tracing in the eight compass directions. Each connected region on the marker image is labeled with a unique ID with the following rules.

i) Pixels in the same region are labeled with the same unique ID.
ii) Different regions are labeled with different ID.

In the seed tracing process, considering that the line between two neighboring pixels in a region should not intersect with object boundary, the seed pixel and its neighboring pixel belong to the same region only if they are both foreground pixels and their common neighboring pixels are not edge pixels at the same time.

D. Labeling Pixels Outside Markers

During labeling the pixels outside the markers, the pixels labeled lastly are more possible to be on the watershed line. To make sure that the edges are labeled as the object boundaries, the gradient image is rectified by assigning the largest gradient magnitude value to the edge pixels first. The unlabeled pixels are processed in a priority value descending order. ST and QU are used to store the unlabeled pixels.

As shown in algorithm (III-D), the priority is processed successively. For each priority level, there are two steps. In the first step, only pixels with priority higher than the current processing priority p_i are processed. These pixels can be divided into two groups. The first group includes pixels with higher priority but not labeled in the previous labeling process, and they are stored in QU. The second includes all the unlabeled pixels with priority p_i. The first group of pixels are processed in advance to the second one. After the first step, if the pixel can not be labeled, it is stored in ST and processed in an reverse order in the second step. If after the second step, the pixel still can not be labeled, it will be stored in QU and processed together with the pixels of which the priority is lower than p_i.

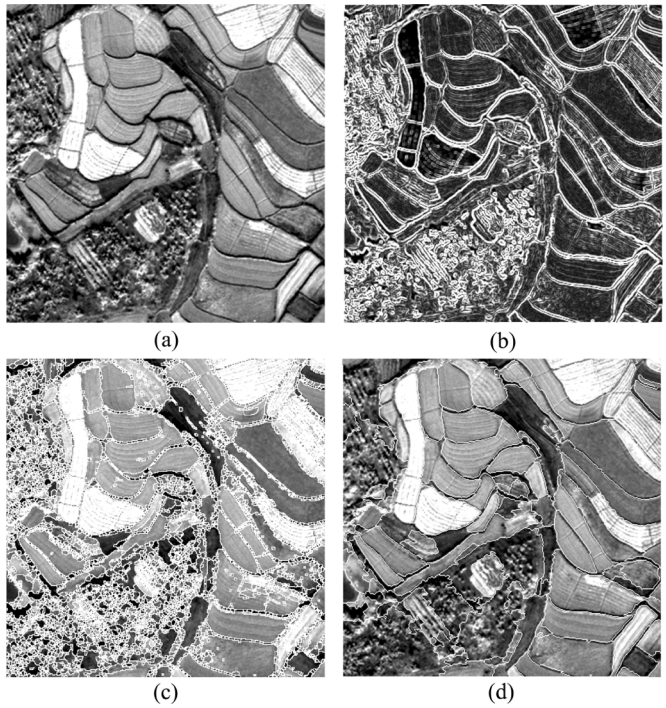

Fig. 3. Experiment I (QuickBird image1). (a) Original image. (b) Gradient image. (c) Segmentation result using H-minima algorithm. (d) Improved marker-based watershed segmentation result.

The labeling operation on pixels outside the markers is dependent upon the number of IDs (n) labeled to the neighboring pixels of the seed pixel. As same as the process of labeling the pixels within the markers, if two pixels are in the same region, their common neighboring pixels should not be edge pixels at the same time. This rule should be obeyed in the counting of the number of the IDs n, the same ID is counted only once, moreover the neighboring pixel is not counted if it breaks the rule.

Algorithm III-D

—labeling pixels outside markers
m: the number of gradient level
i: the current gradient magnitude
Steps:
i) Define the priority of each pixel
ii) Sort the pixels which do not belong to markers in a priority ascending order
iii) Process each pixel according to the priority

for $i = 0$ **to** $m - 1$ **do**

Set the current priority p_i

while QU is not empty **do**

Get the front element p of QU, process the pixel by algorithm III-D1

end while

for all the unlabeled pixels with priority p_i **do**

Process each pixel by algorithm III-D2

end for

while ST is not empty **do**

Get the top element p of ST, process the pixel by algorithm III-D1.

end while

end for

Algorithm III-D1

- labeling pixel p in reverse order

Step: Search all the IDs labeled to the pixels in eight compass directions of p and set n as the number of IDs (the same ID is counted only once)

if $n = 0$ **then**

Push p into ST

else if $n = 1$ **then**

Assign p the ID

else if $n > 1$ **then**

Define p as boundary pixel

end if

Algorithm III-D2

- labeling pixel p in forward order

Step: Search all the IDs labeled to the pixels in eight compass directions of p and set n as the number of IDs

if $n = 0$ **then**

Push p into QU

else if $n = 1$ **then**

Assign p the ID

else if $n > 1$ **then**

Define p as boundary pixel

end if

IV. Experiments

The proposed algorithm is evaluated twofold. A comparison with the state-of-the-art marker-based watershed algorithm namely, H-minima algorithm [1] is conducted. The added value of integrating edge information is demonstrated on two patches of a Quickbird satellite image.

A. Experiment I

The first experiment is applied on a QuickBird remote sensing image with size 400 × 400 [Fig. 3(a)]. It covers a farmland area. Fig. 3(b) is the original gradient image. It can be seen that the inner pixels in objects with complex texture are always with high gradient magnitude, which may result in over-segmentation.

H-minima algorithm [1] is a morphological threshold operator, marking the majority irrelevant small areas as 0. It eliminates the partial minimum that the water basin is lower than the assumed height threshold h. The height threshold h has a direct influence on the segmentation results. The bigger the h is, the less the numbers of the segmented objects are. Empirically, we select 35 as h. In the segmentation result by H-minima algorithm shown in Fig. 3(c), the bushes are over-segmented and there are many unwanted small regions in the farms. In the regional adaptive marker extraction, we empirically determine the optimal parameters: the scale T is set 0.5; the α is set 0.45; area threshold is set 25. The segmentation result is shown in Fig. 3(d). The bushes are partitioned into several regions, and each farm is segmented as one region. Our method can reduce the over-segmentation and get more accurate objects.

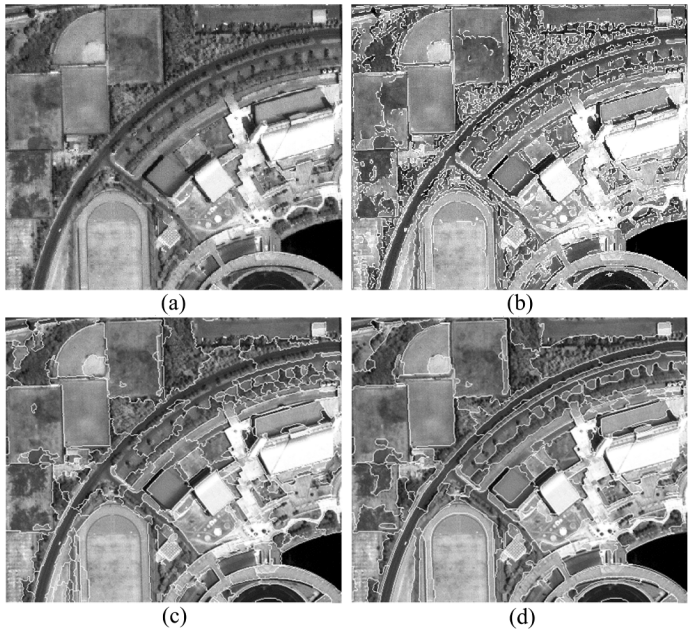

Fig. 4. Experiment II (Quickbird image2). (a) Original image. (b) Edge map detected by the confidence embedded method. (c) Segmentation result by the improved marker-based watershed algorithm. (d) Segmentation result by the improved algorithm integrating the edge information.

B. Experiment II

In this experiment, two QuickBird images are used to demonstrate the added value of integrating edge information. In Fig. 4(a), there are seven main landmarks: road, green belt, play ground, farm, bush, lake and house roof. In Fig. 5(a), there are four main landmarks: road, house roof, forest, and farm. Figs. 4(b) and 5(b) show the edge map detected by the confidence embedded method. Figs. 4(c) and 5(c) show the segmentation without the edge information integrated. Figs. 4(d) and 5(d) show the results integrating the edge information. In Fig. 4(c), road and the green belts nearby it are segmented into one region. In the play ground, we only get a whole region which includes running track and stadium turf. In Fig. 5(c), two farms with weak boundary are labeled into the same region, the road and the trees nearby the road are also labeled in the same region. To conclude, there is under segmentation in Figs. 4(c) and 5(c), and the objects with weak boundaries can not be extracted correctly. Meanwhile, Figs. 4(d) and 5(d) show better segmentation results than those in Figs. 4(c) and 5(c). In Fig. 4(d), the road is segmented out from its neighbor objects and there is a clear boundary between them. The play ground is partitioned into two parts: running track and stadium turf. The small objects, such as single tree, can be extracted correctly. The forest is segmented into a region. In Fig. 5(d), the two farms with weak boundary are segmented into two different regions. At the same time, the road and the trees nearby the road are labeled in different regions.

With assumption that the edge detection embedded with confidence can get accurate edges [17], we can compute the number of boundary

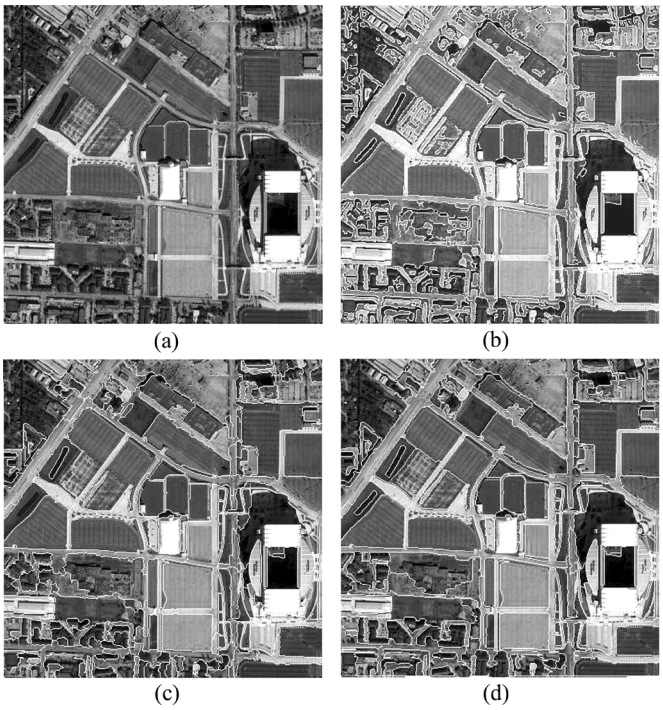

Fig. 5. Experiment II (Quickbird image3). (a) Original image. (b) Edge map detected by the confidence embedded method. (c) Segmentation result by the improved marker-based watershed algorithm. (d) Segmentation result by the improved algorithm integrating the edge information.

TABLE I
NUMBER OF PIXELS

Figure	Boundary pixels	Coincident pixels
4	23814	18501
5	28544	22130

pixels that have the same location as the detected edge pixels and estimate the geometric accuracy of boundary pixels. Table I shows the results. In Fig. 4(d), there are 23814 boundary pixels, 18501 of which coincide with the edge pixels. In Fig. 5(d), there are 28544 boundary pixels, and the number of coincident pixels is 22130. The edge pixels, which do not coincide with boundary pixels, are mostly within the objects which have complex structures. Most of them locate in bushes and green belt. This indicates that the detected edges, which locate in the objects, are not retained in the final segmentation result. Meanwhile, the precise edges that are located between two objects coincide with the object boundaries. To sum up, the proposed segmentation algorithm can solve the under-segmentation problem and retain the accurate boundary.

V. CONCLUSION

An edge embedded marker-watershed image segmentation method is developed for segmenting images with precise objects boundaries and without spurious boundaries. With the edge information detected by the confidence embedded method, the proposed method can be divided into two stages. In the first stage, we extract marker image by binarization. To get good marker image, the threshold of each pixel is defined according to the histogram statistical estimation instead of a single fixed threshold for the whole image. In addition, the edge information is integrated into the extraction of markers with the rule that edges can not cut through a marker. In the second stage, we improve the Meyer's method to label the pixels with only one queue and one stack data structure. The edge information is integrated into the labeling process with the edge pixels assigned the lowest priority and lastly labeled. So the edge pixels become the candidates of the boundary pixels and more precise objects boundaries can be acquired. The two experiments of three QuickBird images show that the proposed regional adaptive marker extraction and the labeling scheme of pixels is effective in reducing over-segmentation. After integrating the edge information, segmentation results are with more precise objects boundaries which coincide with the detected edges quite well. It can be concluded that the method has good generality for integrating edge information into segmentation, and can get good result for images with diverse objects distribution and structure characteristics. Further study is needed to find the way to select the optimal parameter combination for segmentation automatically.

REFERENCES

[1] Y. Sun and G. H. , "Segmentation of high-resolution remote sensing image based on marker-based watershed algorithm," in *Proc. 5th Int. Conf. Fuzzy Systems and Knowledge Discovery*, 2008, pp. 271–276.

[2] T. Blaschke, "Object based image analysis for remote sensing," *ISPRS J. Photogram. Remote Sens.*, vol. 65, no. 1, pp. 2–16, 2010.

[3] N. R. Pal and S. Pal, "A review on image segmentation techniques," *Pattern Recognit.*, vol. 25, no. 9, pp. 1277–1294, 1993.

[4] K. Karantzalos and D. Argialas, "Improving edge detection and watershed segmentation with anisotropic diffusion and morphological levellings," *Int. J. Remote Sens.*, vol. 27, no. 24, pp. 5427–5434, 2006.

[5] Y. Gao, N. Kerle, J. Mas, A. Navarrete, and I. Niemeyer, "Optimized image segmentation and its effect on classification accuracy," presented at the Proc. Int. Symp. Spatial Data Quality, .

[6] Z. Wu, L. Yi, and G. Zhang, "Uncertainty analysis of object location in multi-source remote sensing imagery classification," *Int. J. Remote Sens.*, vol. 30, no. 20, pp. 5473–5487, 2009.

[7] Y. B. Chen and O. T. C. Chen, "Image segmentation method using thresholds automatically determined from picture contents," *J. Image Video Process.*, 2009.

[8] S. Hojjatoleslami and J. Kittler, "Region growing: A new approach," *IEEE Trans. Image Process.*, vol. 7, no. 7, pp. 1079–1084, Jul. 1998.

[9] L. Vincent and P. Soille, "Watersheds in digital spaces: An efficient algorithm based on immersion simulations," *IEEE Trans. Pattern Anal. Mach. Intell.*, vol. 13, no. 6, pp. 583–589, Jun. 1991.

[10] J. Canny, "A computational approach to edge detection," *IEEE Trans. Pattern Anal. Mach. Intell.*, vol. PAMI–8, no. 6, pp. 679–698, Jun. 1986.

[11] F. Shih and S. Cheng, "Adaptive mathematical morphology for edge linking," *Inf. Sci.*, vol. 167, no. 1–4, pp. 9–21, 2004.

[12] W. T. Ma and B. S. Manjunath, "Edge flow: A framework of boundary detection and image segmentation," *IEEE Trans. Image Process.*, vol. 9, no. 8, pp. 1375–1388, Aug. 2000.

[13] R. Trias-Sanz, G. Stamon, and J. Louchet, "Using colour, texture, and hierarchial segmentation for high-resolution remote sensing," *ISPRS J. Photogram. Remote Sens.*, vol. 63, no. 2, pp. 156–168, 2008.

[14] S. Yin and X. Chen, "Reducing boundary effects in image texture segmentation using weighted semivariogram," in *Proc. GeoComputation*.

[15] C. Juan, E. David, and F. Francisco, "Image segmentation based on merging of sub-optimal segmentations," *Pattern Recognit. Lett.*, vol. 27, pp. 1105–1116, 2006.

[16] J. Freixenet, X. Munoz, J. M. D. Raba, and X. Cufi, "Yet another survey on image segmentation: Region and boundary information integration," in *Proc. Eur. Conf. Computer Vision*, 2002, vol. 2352, Lecture Notes in Computer Science, pp. 408–422.

[17] P. Meer and B. Georgescu, "Edge detection with embedded confidence," *IEEE Trans. Pattern Anal. Mach. Intell.*, vol. 23, no. 12, pp. 1351–1365, Dec. 2001.

[18] G. Zhang, Z. Wu, and L. Yi, "Improved marker-based watershed algorithm for segmentation of high spatial resolution remote sensing imagery," *Appl. Res. Comput.*, vol. 27, no. 2, pp. 760–763, 2010.

[19] F. Meyer, "Color image segmentation," in *Proc. IEEE Int. Conf. Image Process. and Its Appl.*, 1992, pp. 303–306.
[20] J. Fan, D. K. Y. Yau, A. K. Elmagarmid, and W. G. Aref, "Automatic image segmentation by integrating color-edge extraction and seeded region growing," *IEEE Trans. Image Process.*, vol. 10, no. 10, pp. 1454–1466, Oct. 2001.
[21] J. F. Haddon and J. F. Boyce, "Image segmentation by unifying region and boundary information," *IEEE Trans. Pattern Anal. Mach. Intell.*, vol. 12, no. 10, pp. 929–948, Oct. 1990.
[22] T. Pavlidis and Y. T. Liow, "Integrating region growing and edge detection," *IEEE Trans. Pattern Anal. Mach. Intell.*, vol. 12, no. 3, pp. 225–233, Mar. 1990.
[23] M. Tabb and N. Ahuja, "Multiscale image segmentation by integrated edge and region detection," *IEEE Trans. Image Process.*, vol. 6, no. 5, pp. 642–655, May 1997.
[24] C. C. Chu and J. K. Aggarwal, "The integration of image segmentation maps using region and edge information," *IEEE Trans. Pattern Anal. Mach. Intell.*, vol. 15, no. 12, pp. 1241–1252, Dec. 1993.
[25] D. Geiger and A. Yuille, "A common framework for image segmentation," *Int. J. Comput. Vis.*, vol. 6, pp. 227–243, 1991.
[26] E. Song, R. Jin, C. C. IIung, T. Luo, and X. Xu, "Boundary refined texture segmentation based on k-views and datagram methods," in *Proc. IEEE Symp. Computat. Intell.*, 2007, pp. 19–23.
[27] L. Gupta, U. G. Mangai, and S. Das, "Integrating region and edge information for texture segmentation using a modified constraint satisfaction neural network," *Image Vis. Comput.*, vol. 26, no. 8, pp. 1106–1117, 2008.
[28] J. L. Moigne and J. C. Tilton, "Refining image segmentation by integration of edge and region data," *IEEE Trans. Geosci. Remote Sens.*, vol. 33, no. 3, pp. 605–615, May 1995.
[29] J. Roerdink and A. Meijster, "The watershed transform: Definitions, algorithms and parallelization strategies," *Fund. Inf.*, vol. 41, pp. 187–228, 2001.
[30] F. Meyer and S. Beucher, "Morphological segmentation," *Vis. Commun. Image Represent.*, vol. 1, no. 1, pp. 21–46, 1990.
[31] P. Karvelis, A. Tzallas, D. Fotiadis, and I. Georgiou, "A multichannel watershed-based segmentation method for multispectral chromosome classification," *IEEE Trans. Med. Imag.*, vol. 27, no. 5, pp. 697–708, May 2008.

On the Complexity of Mumford–Shah-Type Regularization, Viewed as a Relaxed Sparsity Constraint

Boris Alexeev, *Student Member, IEEE*, and Rachel Ward, *Member, IEEE*

***Abstract*—We show that inverse problems with a *truncated quadratic regularization* are NP-hard in general to solve or even approximate up to an additive error. This stands in contrast to the case corresponding to a finite-dimensional approximation to the Mumford–Shah functional, where the operator involved is the identity and for which polynomial-time solutions are known. Consequently, we confirm the infeasibility of any natural extension of the Mumford–Shah functional to general inverse problems. A connection between truncated quadratic minimization and sparsity-constrained minimization is also discussed.**

***Index Terms*—Inverse problems, Mumford–Shah functional, NP-hard, sparse recovery, SUBSET-SUM, thresholding, truncated quadratic regularization.**

I. Introduction

Consider a discrete signal $x \in \mathbb{R}^N$ sampled from a piecewise smooth signal and revealed through measurements $y = Ax + e$, where $e \in \mathbb{R}^m$ is observation noise and $A : \mathbb{R}^N \mapsto \mathbb{R}^m$ is a known linear operator identified with an $m \times N$ real matrix (representing, for instance, a blurring or partial obscuring of the data). Consider the *truncated quadratic minimization problem*

$$\hat{x} = \arg\min_{x \in \mathbb{R}^N} \mathcal{J}(x)$$
$$\mathcal{J}(x) = \|Ax - y\|_2^2 + \sum_{j=1}^{N-1} Q(x_{j+1} - x_j) \tag{1}$$

with truncated quadratic penalty term $Q(u) = \alpha \min\{u^2, \beta\}$ parametrized by $\alpha, \beta > 0$. Since its introduction in 1984 by Geman and Geman in the context of image restoration [1]–[3], this problem has been the subject of considerable theoretical and practical interest, finding applications ranging from visual analysis to crack detection in fracture mechanics [4], [5]. The choice of regularization is motivated as follows: Q desires to smooth small differences $|x_{j+1} - x_j| \leq \sqrt{\beta}$ where it acts quadratically, but suspends smoothing over larger differences.

From a statistical point of view, the quadratic data-fidelity term $\|Ax - y\|_2^2$ can be viewed as a log-likelihood of the data under the hypothesis that e is Gaussian random noise, while the truncated quadratic regularization term corresponds to the energy of a piecewise Gaussian Markov random field [1], [6], [7].

Manuscript received October 27, 2009; revised March 13, 2010; accepted March 13, 2010. Date of publication April 22, 2010; date of current version September 17, 2010. The work of R. Ward was supported in part by the National Science Foundation Postdoctoral Research Fellowship. The wotk of B. Alexeev was supported in part by the National Science Foundation.The associate editor coordinating the review of this manuscript and approving it for publication was Dr. Laurent Younes.

B. Alexeev is with the Department of Mathematics, Princeton University, Princeton, NJ 08544 USA (e-mail: balexeev@math.princeton.edu).

R. Ward is with the Department of Mathematics, Courant Institute of Mathematical Sciences, New York University, New York, NY 10012 USA (e-mail: rward@cims.nyu.edu).

Digital Object Identifier 10.1109/TIP.2010.2048969